doi:10.1016/j.jmb.2007.05.038 J. Mol. Biol. (2007) 371, 210–221

JMB

Available online at www.sciencedirect.com
ScienceDirect

ELSEVIER

A Novel Loop Domain in Superantigens Extends their T Cell Receptor Recognition Site

Sebastian Günther[1]†, Ashok K. Varma[1]†, Beenu Moza[1], Katherine J. Kasper[2] Aaron W. Wyatt[2], Penny Zhu[1], A. K. M. Nur-ur Rahman[2], Yili Li[3] Roy A. Mariuzza[3], John K. McCormick[2] and Eric J. Sundberg[1]*

[1]*Boston Biomedical Research Institute, Watertown MA 02472, USA*

[2]*Department of Microbiology and Immunology University of Western Ontario and the Lawson Health Research Institute, London, Ontario Canada N6A 5C1*

[3]*W.M. Keck Laboratory for Structural Biology Center for Advanced Research in Biotechnology, University of Maryland Biotechnology Institute, Rockville MD 20850, USA*

**Corresponding author*

Superantigens (SAGs) interact with host immune receptors to induce a massive release of inflammatory cytokines that can lead to toxic shock syndrome and death. Bacterial SAGs can be classified into five distinct evolutionary groups. Group V SAGs are characterized by the α3-β8 loop, a unique ~15 amino acid residue extension that is required for optimal T cell activation. Here, we report the X-ray crystal structures of the group V SAG staphylococcal enterotoxin K (SEK) alone and in complex with the TCR hVβ5.1 domain. SEK adopts a unique TCR binding orientation relative to other SAG–TCR complexes, which results in the α3-β8 loop contacting the apical loop of framework region 4, thereby extending the known TCR recognition site of SAGs. These interactions are absolutely required for TCR binding and T cell activation by SEK, and dictate the TCR Vβ domain specificity of SEK and other group V SAGs.

© 2007 Elsevier Ltd. All rights reserved.

Keywords: superantigens; T cell receptor; T cell activity; X-ray crystallography; surface plasmon resonance

Introduction

Bacterial superantigens (SAGs) comprise a large family of disease-associated proteins that are produced primarily by *Staphylococcus aureus* and *Streptococcus pyogenes*.[1] SAGs function by simultaneously interacting with class II major histocompatibility complex (MHC) and T cell receptor (TCR) molecules on antigen presenting cells and T lymphocytes, respectively.[2] Contrary to processed antigenic peptides, SAGs bind to MHC molecules outside of their peptide binding grooves and interact only with the Vβ domains of TCRs, resulting in the stimulation of up to 20% of the entire T cell population. In this way, SAGs initiate a systemic release of inflammatory cytokines that results in various immune-mediated diseases, including a condition known as toxic shock syndrome (TSS) that can ultimately lead to multi-organ failure and death. SAGs have also been classified as Category B Select Agents by the U.S. Centers for Disease Control and Prevention. Despite the intense research efforts that have been directed

† S.G. and A.K.V. contributed equally to this work.

Present addresses: S. Günther, Max-Delbrück-Center for Molecular Medicine, Robert-Rössle-Str. 10, 13125 Berlin, Germany; A.K. Varma, Tata Memorial Centre, Advanced Centre for Treatment, Research and Education in Cancer Kharghar, Navi Mumbai - 410 210, India; A.W. Wyatt, Department of Microbiology and Immunology, University of British Columbia, Vancouver, British Columbia, Canada.

Abbreviations used: CDR, complementarity-determining region; FR, framework region; hVβ2.1, human T cell receptor β chain variable domain 2.1; hVβ5.1, human T cell receptor β chain variable domain 5.1; IL-2, interleukin-2; MHC, major histocompatibility complex; mVβ8.2, murine T cell receptor β chain variable domain 8.2; pMHC, peptide–MHC complex; SAG, superantigen; SEB, staphylococcal enterotoxin B; SEI, staphylococcal enterotoxin I; SEK, staphylococcal enterotoxin K; SpeC, streptococcal pyrogenic exotoxin C; SpeI, streptococcal pyrogenic exotoxin I; SPR, surface plasmon resonance; TCR, T cell receptor; TSS, toxic shock syndrome; TSST-1, toxic shock syndrome toxin-1.

E-mail address of the corresponding author: sundberg@bbri.org

 © 2007 Elsevier Ltd. All rights reserved.

toward the characterization of SAGs, therapeutics capable of neutralizing SAG-mediated T cell activation in humans are clinically unavailable.[3,4]

The binding sites on MHC molecules with which SAGs interact are diverse and can be classified into three distinct groups: (1) a zinc-mediated site on the MHC β subunit that extends over the MHC-bound peptide; (2) a site on the MHC α subunit entirely peripheral to the MHC-bound peptide; and (3) a partially overlapping site on the MHC α subunit that extends over the MHC-bound peptide. Each of these three binding modes has been characterized crystallographically.[5–7] Crystal structures of several SAGs with their respective TCR Vβ ligands have revealed that SAG–Vβ interactions are also structurally diverse.[8–10] These structures have allowed for the construction of models of the ternary MHC–SAG–TCR T cell signaling complexes, which, due to structural diversity in both SAG–MHC and SAG–TCR interactions, exhibit substantially heterogeneous supramolecular architectures, all of which nonetheless allow for efficient T cell activation.

More than 30 distinct SAG serotypes from both staphylococci and streptococci belong to the pyrogenic toxin SAG family.[11] Although they are all believed to share a conserved tertiary structure, five distinct evolutionary groups (I through V) have been proposed for these toxins due to their phylogenetic relationships,[1] and key differences in how the characterized representatives for each group engage their host receptors.[12]

Within this classification, toxic shock syndrome toxin-1 (TSST-1) from *S. aureus* is the only group I SAG and is also unique, in that it binds MHC through an N-terminal, low-affinity binding domain that is peptide-dependent[7,13] and engages the TCR Vβ through two independent regions within both complementarity-determining region (CDR) 2 and framework region (FR) 3,[9] which together exhibit positive cooperative binding.[14] Group II contains both staphylococcal and streptococcal SAGs (including staphylococcal enterotoxin B (SEB), staphylococcal enterotoxin C (SEC), and SpeA) that also bind the MHC α-chain through an N-terminal, low-affinity binding domain; however, in contrast to group I, this binding is peptide-independent.[6] Group II SAGs engage the TCR Vβ through mostly conformation-dependent mechanisms that are largely independent of specific Vβ amino acid side-chains.[8,10,15] Group III SAGs contain only staphylococcal SAGs (such as SEA), and these toxins are able to crosslink MHC molecules[16,17] through a low-affinity site similar to group II,[18] as well as a high-affinity, zinc-dependent MHC binding interface located within the β-grasp domain of the SAG.[19] There is currently little available information regarding how group III SAGs engage Vβ. Group IV SAGs are restricted to only streptococcal members (such as streptococcal pyrogenic exotoxin C (SpeC)), and these toxins contain a high-affinity MHC binding domain similar to that of group III.[20] The structure of SpeC in complex with human T cell receptor β chain variable domain 2.1 (hVβ2.1) revealed that this SAG engages each of the TCR Vβ hypervariable loops, including each of CDR loops 1 through 3 and HV4.[8] On the basis of these collective characteristics, it is clear that the SAG evolutionary groups I through IV each display key differences in how they engage their host receptors.

Group V SAGs (including streptococcal pyrogenic exotoxin I (SpeI), SEI and staphylococcal enterotoxin K (SEK)) are the least characterized of all of these toxins. A crystal structure of SEI in complex with HLA-DR1 showed that this group of SAGs binds to class II peptide–MHC complex (pMHC) molecules in a fashion similar to that of group IV SAGs.[21] A key feature of group V SAGs is the presence of a loop extension between the third α-helix and the eighth β-sheet, referred to as the α3-β8 loop. This ∼15-amino acid residue extension is not found in the other SAG groups,[1] and is not involved in pMHC interactions. Instead, we have shown recently that the α3-β8 loop of SpeI is functionally important for the activation of T cells.[12] In particular, the presence of several Gly residues within this loop is necessary for optimal T cell stimulation, suggesting that flexibility and/or the ability to adopt an otherwise unattainable conformation are key structural features of this loop.

In order to further define the functional relevance of the α3-β8 loop unique to group V SAGs, we have undertaken structural, energetic and functional analyses of SEK binding to one of its known TCR ligands, the human Vβ domain 5.1 (hVβ5.1). Here, we report the X-ray crystal structures of SEK alone, as well as in complex with hVβ5.1. These structures show that the conformation of the loop is not altered upon TCR binding. Residues within the α3-β8 loop make intermolecular contacts with hVβ5.1 and extend the known TCR Vβ domain binding site for SAGs into the FR4 region. Using surface plasmon resonance (SPR) molecular interaction analysis and functional assays employing an engineered hVβ5.1$^+$ Jurkat T cell line, we document the functional importance of these contact residues. The SEK-hVβ5.1 crystal structure shows also that SEK adopts a distinct orientation in binding the TCR Vβ domain relative to other SAG–TCR interactions. As a result, the majority of the interface comes from a contiguous stretch of residues comprising the SEK N terminus and the α1 α-helix.

Results

SEK is structurally homologous to other group V superantigens

We have determined the X-ray crystal structure of SEK in its unbound state (Figure 1(a)). The crystal was grown with a single-site mutant of SEK, SEK-C73S, in which the sole cysteine residue in SEK was mutated to serine in order to reduce disulfide-linked aggregation and promote crystallization. This residue lies outside of the molecular interface formed with hVβ5.1 (see below) and does not affect SEK structure or function in any detectable way. The structure was solved by molecular replacement methods using the structure of SpeI as a model.[12]

The structure has been refined to a resolution of 1.56 Å. Data collection, processing and refinement statistics are given in Table 1.

The structure of SEK conforms to the classical bacterial SAG fold that is comprised of N-terminal β-barrel and C-terminal β-grasp domains. All residues in the structure exhibited unambiguous electron density, including the α3-β8 loop. The conformation of this loop is very similar to the analogous loops of SEI and SpeI (Figure 1(b)), two other group V SAGs for which crystal structures have been determined. The structure of the putative MHC binding site on SEK is also structurally homologous to that of SEI (Figure 1(c)), and thus, SEK likely binds to MHC in a fashion similar to that of the latter.[21] The zinc-dependence of SEK binding to the high-affinity MHC class II binding site was confirmed by an aggregation assay using LG-2 antigen presenting cells (data not shown).

The conformation of the α3-β8 loop does not change upon TCR binding

We have determined the X-ray crystal structure of SEK bound to its TCR Vβ domain ligand hVβ5.1 (Figure 2(a)). This structure was solved by molecular replacement methods using the structures of SEK in the unbound state and of the β-chain of the 3A6 TCR,[22] refined to a resolution of 2.4 Å. Data collection, processing and refinement statistics for this structure are given in Table 1. Characterization of the SEK-hVβ5.1 molecular interface reveals that it is more akin to those SAG–TCR complexes formed by group I (i.e. TSST-1) and group IV (i.e. SpeC) SAGs than by group II (i.e. SEB) SAGs, in terms of intermolecular contacts, buried surface area and shape complementarity (Table 1).

Our recent structural and functional analysis of the group V SAG SpeI showed that the α3-β8 loop of this SAG, and by analogy those of other Group V SAGs, was necessary for optimal T cell activation.[12] In the unbound structure of SpeI, the α3-β8 loop is well ordered, built into unambiguous electron density and exhibits relatively low temperature factors, but is also glycine-rich. Thus, we propose that one possible mechanism by which this loop contributes to TCR engagement was through conformational changes induced upon binding. A comparison of the α3-β8 loop in SEK when bound or not to hVβ5.1, however, shows that this loop is conformationally unchanged (Figure 2(b)). There is essentially no main chain or side-chain movement between the unbound and the bound states of SEK. Thus, the α3-β8 loop of SEK is pre-ordered in a conformation that is amenable for TCR engagement.

The TCR recognition site for superantigens is extended by the α3-β8 loop

Two distinct regions of SEK, the α3-β8 loop and the N terminus, form intermolecular contacts with hVβ5.1. Only two residues within the α3-β8 loop, His142 and Tyr158, contact TCR, and each of these exhibits both hydrogen bonding and van der Waals interactions with residues in hVβ5.1 (Figure 2(c)). Surprisingly, these contacts are made to residues in the apical loop of FR3, which we predicted from our previous analysis of SpeI,[12] and with residues in the apical loop of FR4. This is the first time that this region of the TCR has been implicated in SAG binding. Additionally, a contiguous stretch of residues forming the N terminus of SEK at positions 1–16, make a variety of hydrogen bonding and van der Waals interactions with hVβ5.1 exclusively from the CDR2 loop (Figure 2(d)).

SEK adopts a unique TCR binding orientation relative to that of other SAG–TCR complexes

SEK adopts a unique orientation when engaging the TCR Vβ domain relative to representative SAGs from groups I, II and IV (Figure 3(a)). Like TSST-1, SEK, due to the extension by the α3-β8 loop, is positioned higher (i.e. closer to the Cβ domain) on the Vβ domain than are SEB and SpeC (Figure 3(a), upper panels). Despite its higher position on the Vβ domain, SEK is aligned in the same plane as are SEB and SpeC, whereas TSST-1 is rotated by approximately 45° (Figure 3(a), lower panels).

The distinct orientations with which each of these representative SAGs from groups I, II, IV and V engage the TCR Vβ domain result in unique patterns of hypervariable and framework region surfaces that are buried (Figure 3(b)). Binding to the TCR Vβ CDR2 loop is a requirement for all bacterial SAGs, and the proportion of the SAG–TCR interface that is contributed by the CDR2 loop is invariably the greatest in any SAG–TCR complex, relative to any other single hypervariable or framework region. In this way, SEK is similar to other SAGs. When the group V SpeI crystal structure is superimposed onto the SEK-hVβ5.1 crystal structure, SpeI residues Asn13, Ser77 and Arg198, all of which were shown to be important for human T cell proliferation,[12] surround the CDR2 loop.

Involvement of Vβ domain regions beyond the CDR2 loop, however, plays a significant role in the TCR Vβ domain specificity and cross-reactivity of a SAG (Figure 3(b)).[14,23,24] SEK and TSST-1, due to their higher position on the Vβ domain, engage one or more framework region apical loops, at the expense of contacting the hypervariable elements. SEK buries significant molecular surface belonging to both the FR3 and FR4, while TSST-1 contacts only residues from FR3. The lower relative positions of SEB and SpeC on the Vβ domain result in their engagement of hypervariable elements at the expense of binding the apical loops of the framework regions. SEB buries molecular surface belonging to HV4, while SpeC contacts residues from CDR1, CDR3 and HV4.

Contact residues in the α3-β8 loop are required for TCR binding

Using SPR analysis, we determined the affinity of the wild-type SEK-hVβ5.1 complex to be 6 μM

(Figure 4(a)). This is within the range of affinities (10^{-7}–10^{-4} M) of all known SAG–TCR interactions.

In order to determine whether the intermolecular contacts made by residues in the α3-β8 loop that we observed in our SEK-hVβ5.1 crystal structure are energetically significant, we analyzed by SPR the capacity of SEK variants with mutations at either His142 or Tyr158 to bind hVβ5.1. His 142 makes three hydrogen bonds (one of which is to the hVβ5.1 main chain) and three van der Waals contacts with residues

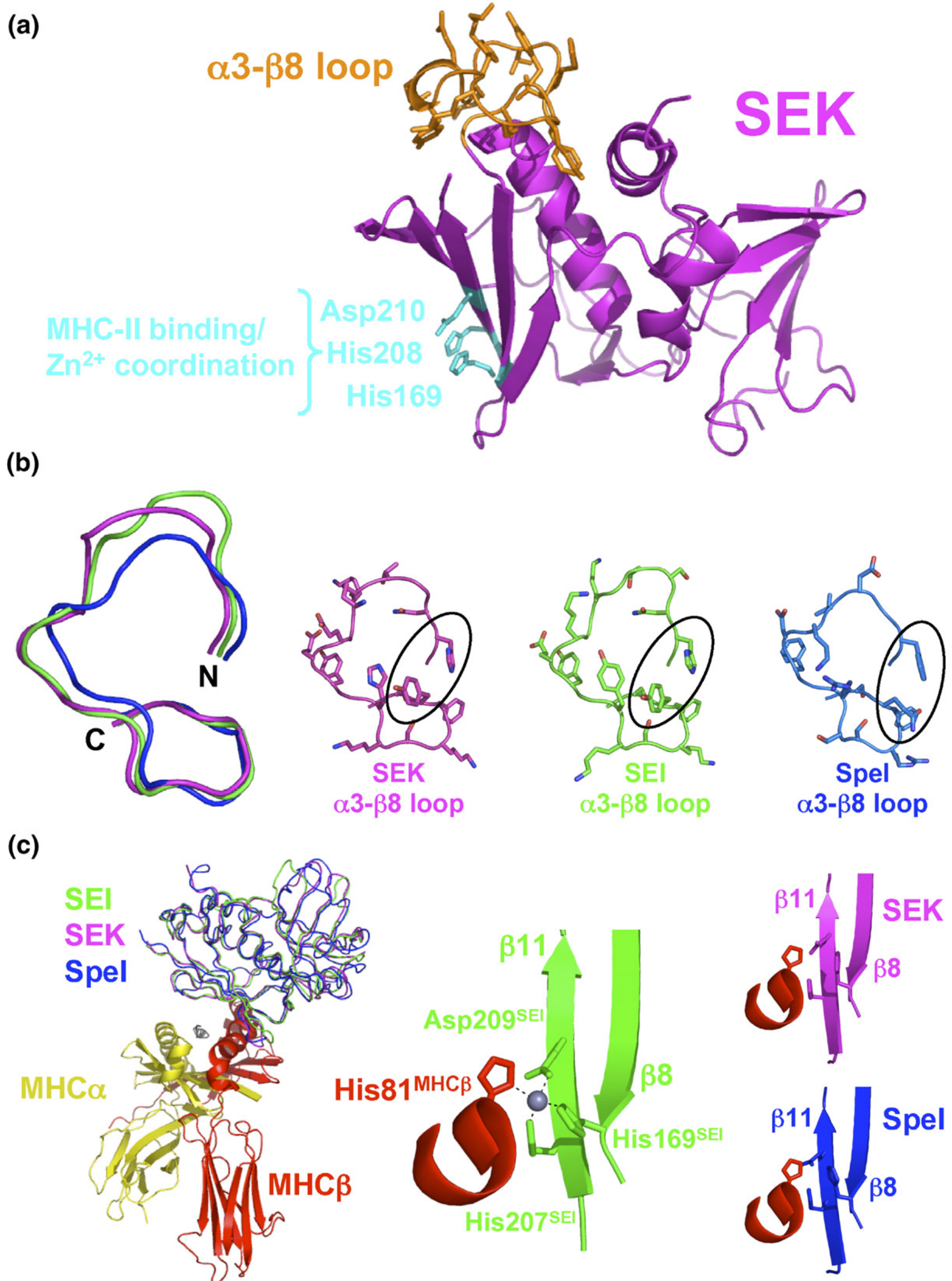

Figure 1 (*legend on next page*)

Table 1. Structure determination and refinement statistics

	SEK	SEK–hVβ5.1
A. *Data collection and processing*		
Space group	$P2_1$	$P2_12_12_1$
Resolution (Å)	1.56	2.40
Molecules/asymmetric unit	2 SEK	1 SEK/1 hVβ5.1
Observations	226,878	176,078
Unique reflections	63,074	21,526
Completeness (%)[a]	99.8 (99.0)	99.9 (100.0)
Redundancy[a]	3.6 (2.8)	8.2 (7.9)
R_{sym} (%)[b]	8.6 (17.9)	8.7 (34.1)
Mean $I/\sigma(I)$	30.9 (5.9)	25.9 (6.1)
B. *Refinement*		
R_{cryst} (%)[c]	16.3	21.9
R_{free} (%)[d]	20.2	24.0
Protein residues	434	462
Average *B* values		
SEK ($Å^2$)	9.9	32.8
hVβ5.1 ($Å^2$)		37.7
Water molecules	655	152
Ramachandran plot		
Core (%)	87.0	84.5
Allowed (%)	12.2	13.5
Generously allowed (%)	0.8	0.7
Disallowed (%)	0	1.2[e]
RMSD from ideality		
Bond lengths (Å)	0.008	0.007
Bond angles (deg.)	1.23	1.69
C. *Molecular characterization*		
Intermolecular contacts		
Hydrogen bonds		14
van der Waals interactions		75
Buried surface areas		
ΔASA_{total} ($Å^2$)		1572
ΔASA_{polar} ($Å^2$)		920
ΔASA_{apolar} ($Å^2$)		658
$\Delta ASA_{apolar}/\Delta ASA_{polar}$ (%)		42
S_C		0.70

[a] Values in parentheses are for the highest resolution shell: 1.62–1.56 Å for SEK; 2.49–2.40 Å for SEK-hVβ5.1.
[b] $R_{sym} = \sum|((I_{hkl} - I_{(hkl)})|/(\sum I_{hkl})$, where $I_{(hkl)}$ is the mean intensity of all reflections equivalent to *hkl* by symmetry.
[c] $R_{cryst} = \sum||F_o| - |F_c||/\sum|F_o||$, where F_c is the calculated structure factor.
[d] R_{free} is calculated as R_{cryst} using 5.1% (SEK) and 4.7% (SEK-hVβ5.1) of the reflections chosen randomly and omitted from the refinement calculations.
[e] Residues in the disallowed region include Ser134$^{hV\beta5.1}$, Ala136$^{hV\beta5.1}$, Thr202$^{hV\beta5.1}$, Glu225$^{hV\beta5.1}$, and Ser73^{SEK}.

in both the apical loops of FR3 and FR4 of hVβ5.1 (Figure 2(c)). An alanine mutation at this position completely abrogated binding to hVβ5.1 (Figure 4(b), left-hand panel). Tyr158 makes a single hydrogen bond and ten van der Waals contacts to residues in the apical loop of the hVβ5.1 FR4 (Figure 2(c)). An alanine mutation at this position also resulted in no hVβ5.1 binding (Figure 4(b), middle panel). A phenylalanine mutation of Tyr158, which removes the hydrogen bond formed between the hydroxyl groups of Tyr158^{SEK} and Thr78$^{hV\beta5.1}$, as well as a single van der Waals contact, showed minimal SPR responses at higher concentrations (up to 50 μM, ~10-fold the wild-type K_D; Figure 4(b), right-hand panel), indicating dramatically reduced binding.

The α3-β8 loop contact residues are functionally critical

In order to verify the functional importance of the α3-β8 loop for the activation of T cells, we performed stimulation assays using an engineered hVβ5.1$^+$ Jurkat T cell line with the wild-type and mutant SEK molecules. The functional responses (Figure 4(c)) for wild-type SEK, SEK(H142A), SEK(Y158A) and SEK (Y158F) all corroborate the results of the SPR binding analysis. As expected, wild-type SEK produced significant dose-dependent secretion of interleukin-2 (IL-2) starting at concentrations as low as 100 pg/ml. T cell stimulation by both of the alanine mutants of His142 and Tyr158 resulted in very little production of IL-2, even at concentrations as high as 10 μg/ml. In accordance with the reduced, but not fully abrogated, binding of the SEK(Y158F), T cell stimulation by this mutant resulted in significant production of IL-2 at concentrations as low as 1 ng/ml, albeit diminished relative to wild-type SEK.

The SEK-dependent T cell signaling complex

In order to activate T cells, SAGs must bind simultaneously to both MHC class II molecules and TCRs. By superimposing SAG–MHC and SAG–TCR X-ray crystal structures, models of MHC–SAG–TCR ternary signaling complexes have been generated for TSST-1,[7,9] SEB,[6,10] and SpeC,[5,8] representative SAGs for group I, II and IV SAGs, respectively (Figure 5(a)–(c)). Using the SEK and SEK-hVβ5.1 complex structures reported here, we have generated a model of the MHC-SEK-TCR T cell signaling complex (Figure 5(d)), which is likely representative of all group V SAGs. The supramolecular architecture of this SEK-dependent ternary complex is very similar to that made by SpeC. Because SEK engages the TCR Vβ domain such that it can bind to the FR apical loops, while SpeC engages the Vβ domain

Figure 1. Structural similarity of SEK and other group V bacterial superantigens. (a) Structure of SEK in the unbound state. The α3-β8 loop is in orange and the residues responsible for Zn^{2+} coordination and MHC class II binding are in cyan. (b) Structural comparison of the α3-β8 loop domains of SEK, SEI and SpeI. Superposition of the main chains of the α3-β8 loops (left-hand panel). Molecular details of side-chain positions in the α3-β8 loops (right-hand panels). SEK, SEI and SpeI are in magenta, green and blue, respectively. The residues in SEK that interact with TCR, His142 and Tyr158, as well as corresponding residues in SEI and SpeI are encircled. (c) Structural comparison of the MHC binding site of SEI and the putative MHC binding sites of SEK and SpeI. Superposition of SEK and SpeI with SEI from the SEI-MHC class II crystal structure (left-hand panel).[21] Close-up view of the Zn^{2+} coordination between SEI residues His169, His207 and Asp209 and the MHC β subunit residue His81 (middle panel). Close-up views of the putative SAG-MHC interface formed by the superposed SEK and SpeI structures (right-hand panels). The MHC α subunit is in yellow, the MHC β subunit is in red, the zinc ion is in gray, and the SAG colors are as in (b).

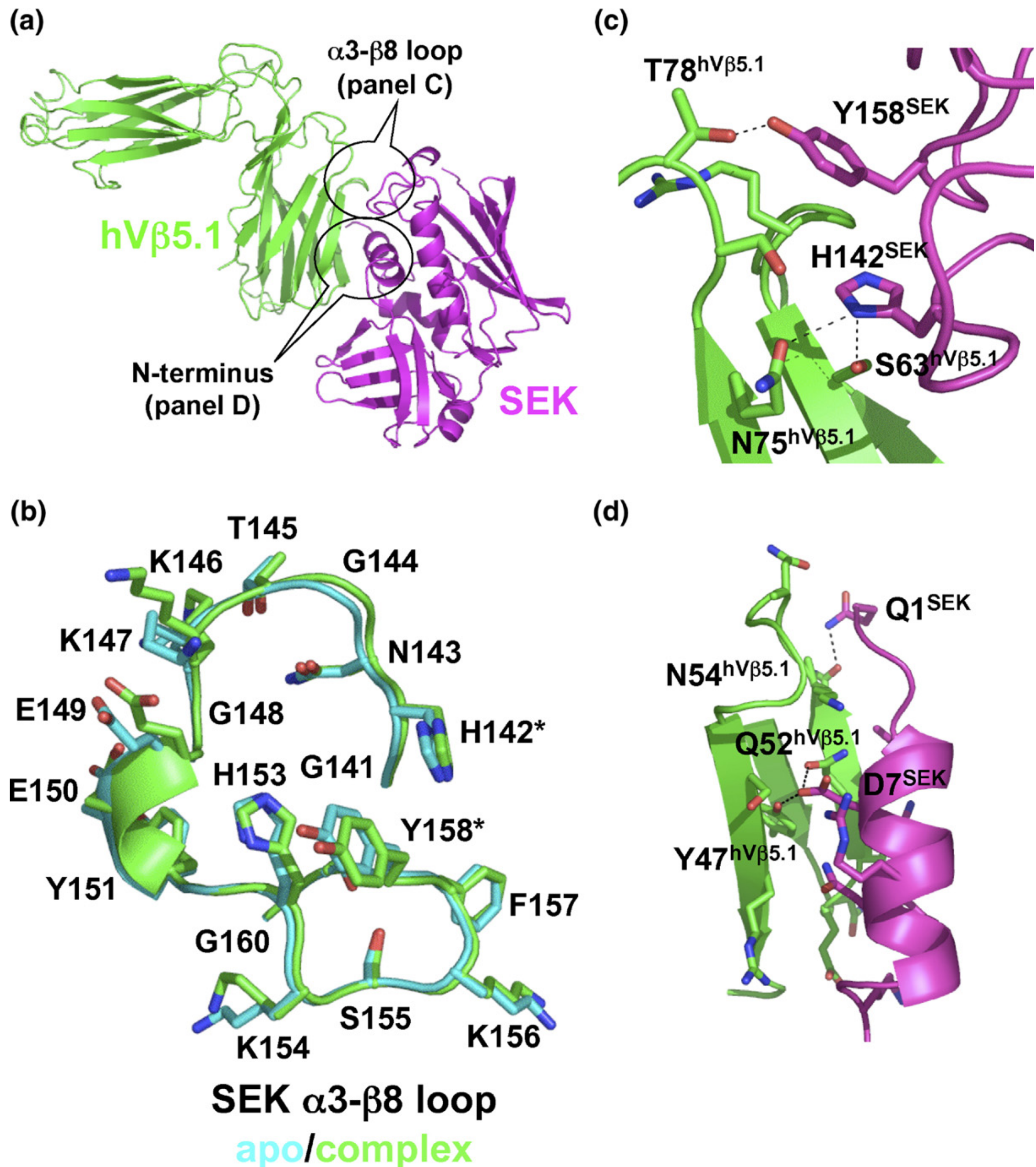

Figure 2. Structure of the SEK-hVβ5.1 complex. (a) Cartoon representation of the interaction between SEK and hVβ5.1. SEK is in magenta, hVβ5.1 is in green. The two regions of SEK, the α3-β8 loop and the N terminus, which contact the TCR, are encircled. (b) Comparison of SEK α3-β8 loop structures in the unbound (cyan) and hVβ5.1-bound (green) crystal structures. The residues that make intermolecular contacts with hVβ5.1, His142 and Tyr158, are indicated by asterisks. (c) Close-up view of the interface formed by the α3-β8 loop of SEK and the FR3 and FR4 loops of hVβ5.1. (d) Close-up view of the interface formed by the N terminus of SEK and the CDR2 loop of hVβ5.1. In (c) and (d), the side-chains of only the residues that make intermolecular contacts are shown, and side-chain to side-chain hydrogen bonds are shown as broken lines.

such that it binds all of the CDR loops, the angle formed between the axis of the MHC-displayed peptide and the long axis the TCR Vβ domains is more acute in the SEK-dependent versus SpeC-dependent complexes (i.e. these axes are approximately 25° closer to parallel in the SEK-dependent ternary complex than in the SpeC-dependent ternary complex).

Discussion

The activation of T cells by SAGs is dependent on both their interactions with MHC class II and TCR molecules. The manner in which SAGs bind to MHC has been investigated in great detail,[5–7] and it is now clear that these interactions are restricted to three distinct binding modes: (1) a zinc-

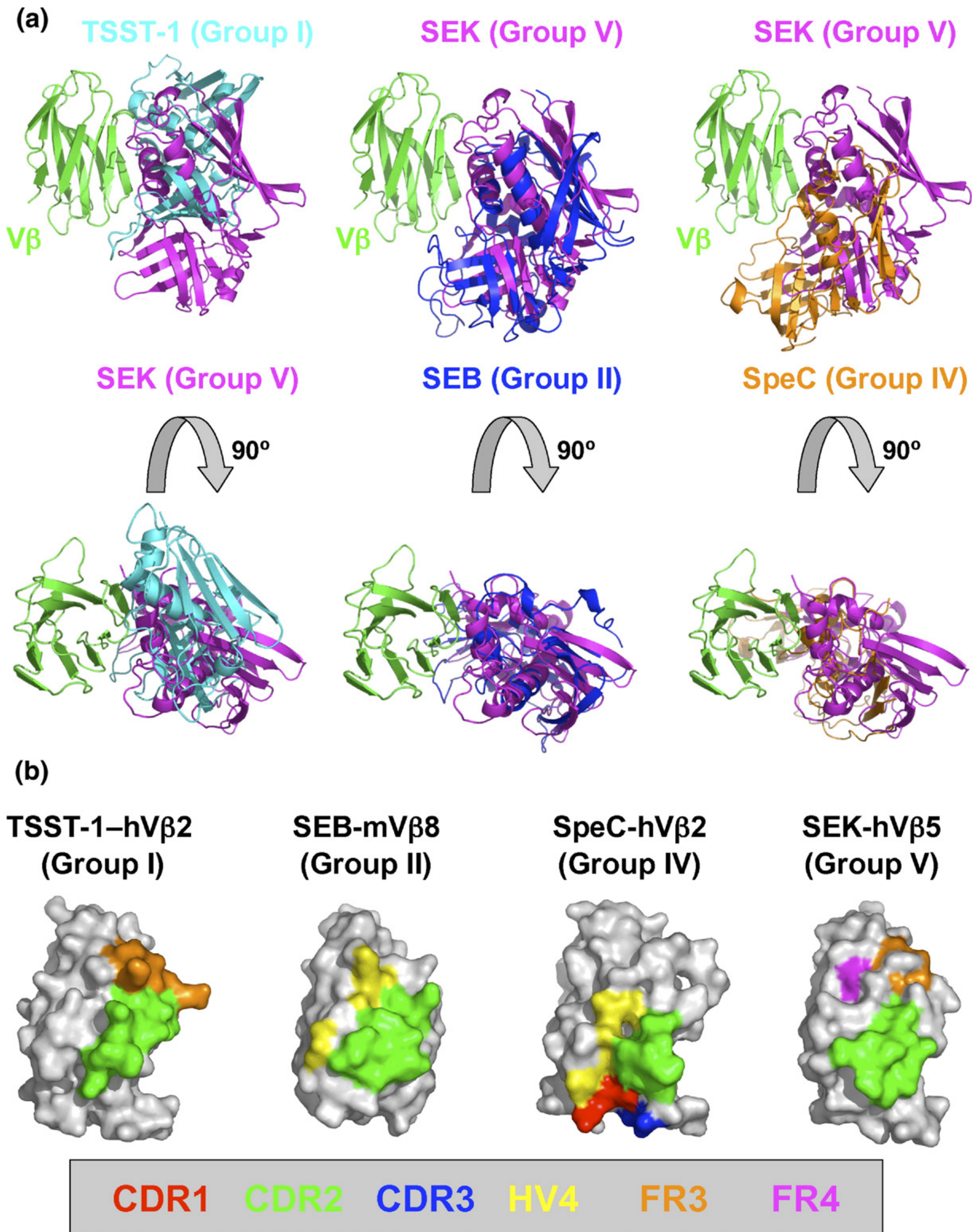

Figure 3. Diverse TCR engagement by bacterial SAGs. (a) Superposition of the SEK-hVβ5.1 crystal structure with the TSST-1–hVβ2.1 (left-hand panels), SEB-mVβ8.2, murine T cell receptor β chain variable domain 8.2 (mVβ8.2) (middle panels) and SpeC-hVβ2.1 (right-hand panels) complexes. The hVβ2.1 and mVβ8.2 molecules have been removed for clarity. SEK is in magenta, TSST-1 is in cyan, SEB is in blue, SpeC is in orange and Vβ is in green. (b) TCR Vβ domain molecular surface buried by various SAGs. Hypervariable and framework region surface residues buried in the interface formed by TSST-1, SEB, SpeC and SEK are color-coded as follows: CDR1, red; CDR2, green; CDR3, blue; HV4, yellow; FR3, orange; and FR4, magenta. The total buried surface areas for each SAG-TCR complex are: TSST-1–hVβ2.1, 1917 Å^2;[9] SEB-mVβ8.2, 1268 Å^2;[10] SpeC-hVβ2.1, 1818 Å^2;[8] and SEK-hVβ5.1, 1572 Å^2.

mediated site on the MHC β subunit that extends over the antigenic peptide; (2) a site on the MHC α subunit entirely peripheral to the displayed peptide; and (3) a partially overlapping site on the MHC α subunit that extends over the MHC-bound peptide.

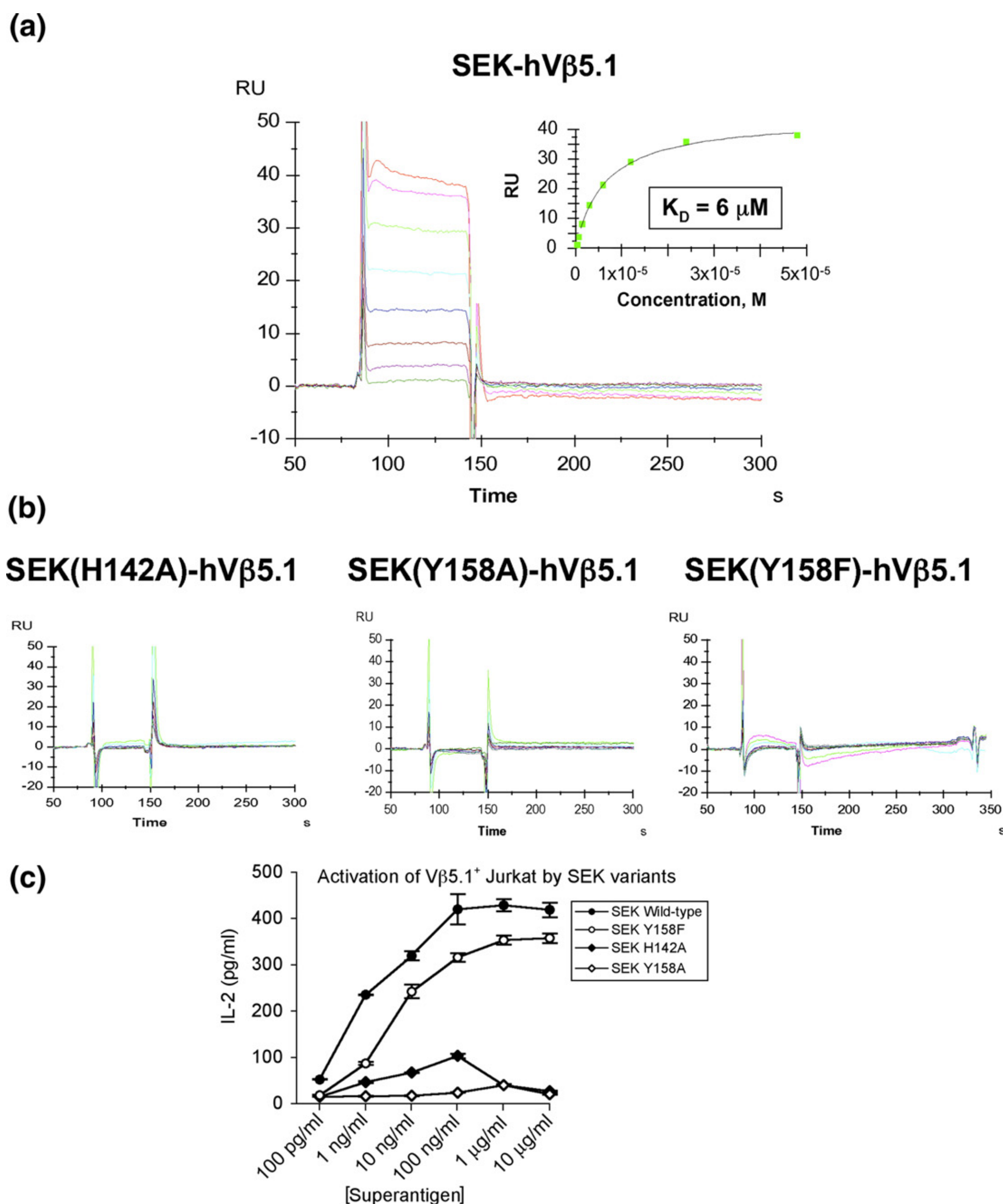

Figure 4. Analysis of SEK-hVβ5.1 binding and SEK-mediated T cell activation. (a) SPR analysis of the wild-type SEK-hVβ5.1 interaction. Non-linear regression analysis of maximal responses *versus* concentration is shown in the inset plot. (b) SPR analyses of hVβ5.1 interactions with the SEK(H142A), SEK(Y158A) and SEK(Y158F) mutants. (c) IL-2 secretion by eJRT3-5.1 cells incubated with various concentrations of wild-type SEK and the SEK(H142A), SEK(Y158A) and SEK(Y158F) mutants presented by LG-2 cells. The data shown are the average±SEM.

There appears to be even greater diversity in the way that SAGs engage TCR (Figure 3(a)). While each SAG–TCR complex investigated by structural analysis to date involves extensive SAG contacts with the CDR2 loop of the TCR, representative SAGs from each SAG group contact distinct combinations of hypervariable and framework regions that contribute to these SAG–TCR interfaces. Moreover, the interactions outside the CDR2 loop have been shown to be important for the TCR specificity of individual SAGs.[14,23,24]

The structural analysis of SEK (Figure 1) and its complex with hVβ5.1 (Figure 2) presented here reveal that SEK is no different in this sense. As a representative of group V SAGs, SEK engages its TCR Vβ domain ligand in a manner distinct from that of representatives of group I, II, and IV SAGs (Figure 3). In particular, SEK makes intermolecular contacts with residues in the apical loops of both FR3 and FR4, the latter of which has not been observed to play a role in SAG-TCR interactions before, and was not known to have any effect on the SAG-mediated activation of T cells.

The molecular surface of hVβ5.1 belonging to FR4 that is buried by SEK makes numerous hydrogen bonds and van der Waals interactions with two

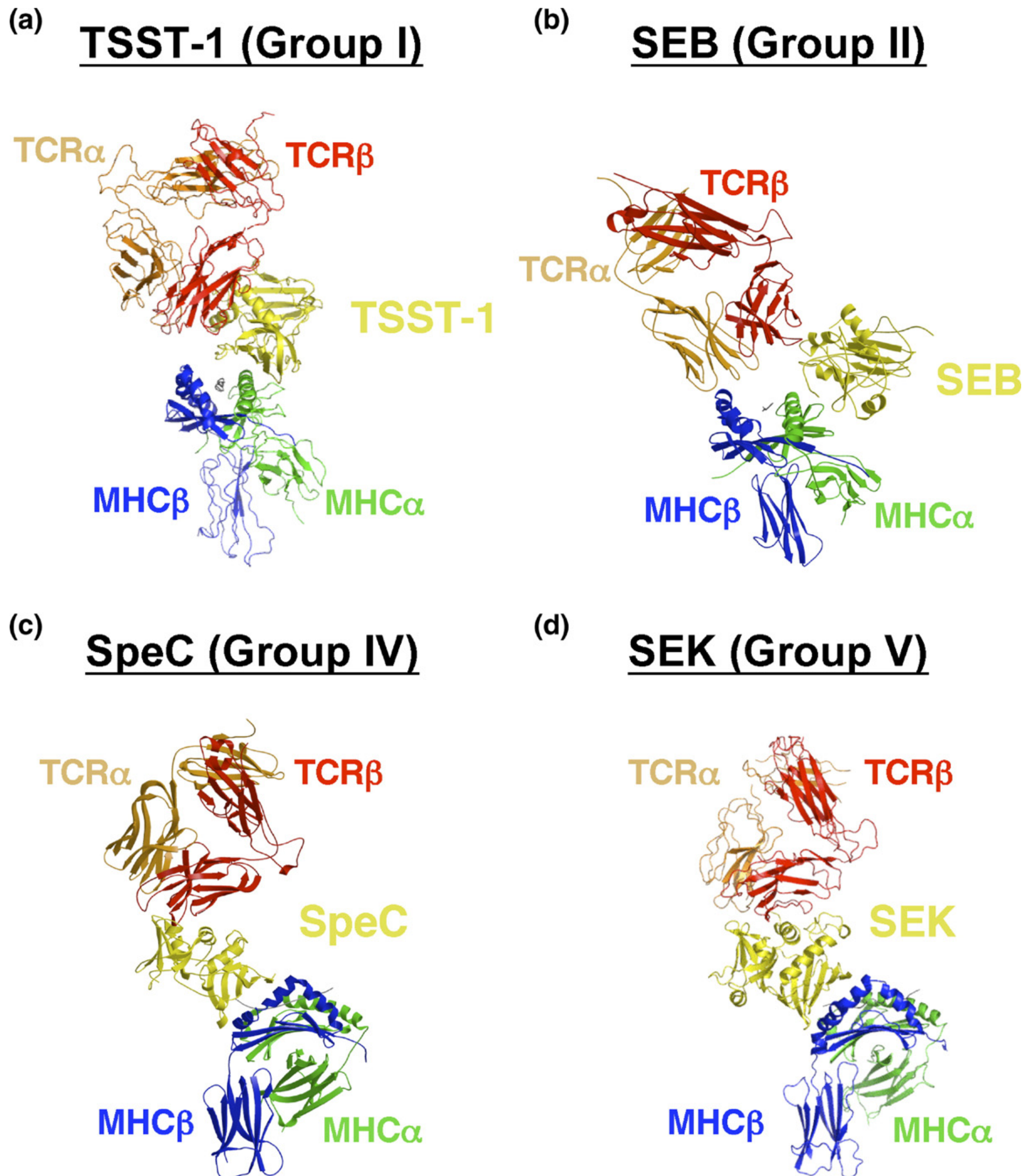

Figure 5. MHC-SAG-TCR ternary signaling complexes mediated by (a) TSST-1, (b) SEB, (c) SpeC, and (d) SEK. Colors are as follows: MHC α subunit, green; MHC β subunit, blue; antigenic peptide, gray; TCR α chain, orange; TCR β chain, red; SAGs, yellow. For clarity, the MHC-SAG-TCR complexes mediated by (c) SpeC and (d) SEK are rotated approximately 90° clockwise about the vertical axis of the page relative to those mediated by (a) TSST-1 and (b) SEB.

residues, His 142 and Tyr158, in the α3-β8 loop of SEK. Our previous studies implicated the α3-β8 loop, which is unique to group V SAGs, as being required for the efficient activation of T cells.[12] Indeed, binding and functional analyses of wild-type and mutant SEK presented here (Figure 4) show that each of these two residues in the SEK α3-β8 loop is absolutely critical for stimulation of hVβ5.1$^+$ T cells.

Beyond being required for the SEK-hVβ5.1 interaction, contacts between the group V α3-β8 loop and Vβ FR4 residues appear to dictate the TCR Vβ specificity of these SAGs. The α3-β8 loops of SEK and SEI are essentially identical in conformation, and both of these SAGs have the same Vβ-contacting His and Tyr residues at positions 142 and 158, respectively (Figure 1(b)). SEI, like SEK, stimulates predominantly hVβ5.1$^+$ T cells.[25] SpeI, conversely, does not stimulate hVβ5.1$^+$ T cells, even though this group V SAG is highly homologous to both SEK and SEI.[12] While the positions of SpeI residues that are analogous to those at positions 142

and 158 of SEK are superimposable, these two residues are Phe and Gln in SpeI (Figure 1(b)).

This extension of the TCR recognition site to FR4 through critical contacts with SEK α3-β8 loop residues provides essential data with which to refine our understanding of SAG-TCR specificity and cross-reactivity. Crystal structures of SEB, SpeA and SpeC with their TCR ligands have shown that TCR increased specificity for these SAGs correlates with the amount of buried surface, the number of side-chain to side-chain hydrogen bonds, the engagement of increasing numbers of CDR loops and the targeting of CDR loops that have incorporated non-canonical residue insertions.[8,10] The recent crystal structure of TSST-1, the most specific SAG known, bound to hVβ2.1, its sole TCR ligand, showed that TSST-1 derives its specificity primarily by targeting unique residues within the apical loop of FR3, at the expense of contacting any CDR loop other than CDR2.[9]

Likewise, SEK, which activates T cells bearing primarily hVβ5.1, as well as hVβ5.2 and hVβ6.7,[26] appears to derive its specificity, at least in part, through interactions with residues in FR3 and FR4; namely, at positions 63 and 75, with which His142 forms side-chain to side-chain hydrogen bonds (Figure 2(c)). These include a serine residue at position 63 in all three of these Vβ domains and either an asparagine residue in hVβ5.1 and hVβ5.2 or a threonine residue in hVβ6.7, which can presumably satisfy the same hydrogen bonding constraints as those observed in the SEK-hVβ5.1 complex structure. The SEK-Vβ domain interfaces are extensive (1572 $Å^2$ for the SEK–hVβ5.1 complex), however, and the numerous other residues within these interfaces are likely to contribute significantly to both binding and specificity. Only an extensive mutagenesis, structural and energetic analysis would allow for the determination of the molecular basis of the fine specificity of SEK-Vβ domain interactions, such as we have done for TSST-1–Vβ and SpeC-Vβ interactions.[9,14,24]

TCR hVβ5 and hVβ6 domains, and especially hVβ5.1, have been shown to be over-represented in patients with Crohn's disease, a severe inflammatory bowel syndrome.[27] These TCRs are over-represented also in juvenile arthritis and periodontitis.[28,29] Other than the SAGs that belong to group V, only SEE, a group III SAG, stimulates $hVβ5.1^+$ T cells. However, with no α3-β8 loop, the orientation of SEE on hVβ5.1 is likely to be markedly different than that of SEK, and the interaction is unlikely to involve the FR3 and FR4 apical loops of the Vβ domain. No other SAG is known to stimulate $hVβ5.2^+$ or $hVβ6.7^+$ T cells.

The unique binding orientation, relative to other SAG–TCR complexes, by which SEK interacts with hVβ5.1 has two important ramifications for T cell activation. First, it results in several regions of both SEK and hVβ5.1 that are not involved in any other SAG–TCR complex, including the N terminus and the α3-β8 loop of the former and residues in FR4 of the latter, forming the majority of the molecular interface. Second, the MHC–SAG–TCR signaling complex mediated by SEK, although more similar to that of SpeC than of other SAGs due to their common interaction with MHC class II molecules, exhibits a different relative juxtaposition of the TCR and MHC molecules. The recent discovery of a Gα11-dependent T cell signaling pathway used by SAGs that is distinct from the Lck-dependent pathway used by antigenic peptide-MHC complexes suggests that SAGs can use a G protein-coupled receptor as a co-receptor on T cells.[30] Thus, the relative orientations of SAG, MHC and TCR in SAG-mediated signaling complexes that we observe in the MHC–SEK–TCR ternary complex may have significant functional consequences for the engagement of this co-receptor and subsequent triggering of this alternative and SAG-specific T cell signaling pathway.

Materials and Methods

Protein production

Like SpeI, SEK contains a single cysteine residue that promotes a monomer–dimer equilibrium at protein concentrations needed for crystallization. It had been observed for SpeI that mutation of its cysteine residue to serine resulted in the growth of diffraction-quality crystals,[12] and thus, an identical strategy was followed for SEK mutagenesis, expression, purification and crystallization. Briefly, a C73S mutant of SEK was made following the QuikChange site-directed mutagenesis protocol (Stratagene). SEK-C73S was cloned into a modified pET28a expression vector (Novagen), in which the enterokinase cleavage site had been replaced by a tobacco etch virus (TEV) cleavage site leaving the N-terminal His_6 purification tag intact, expressed in *Escherichia coli* BL21(DE3) cells, and purified on a nickel affinity column. Recombinant, auto-inactivation-resistant His_7::TEV was used to cleave the His6::SEK-C73S fusion protein, and the cleaved purification tag and the His_7::TEV were removed by an additional passage over the nickel affinity column. The resulting product, which contained no extra residue on either terminus, was further purified by size-exclusion chromatography in 10 mM Tris–HCl (pH 7.5), 25 mM NaCl. For SEK-hVβ5.1 co-crystallization and binding analysis, the SEK-C73S mutant described above was used and the TCR β chain from the 3A6 TCR (hVβ5.1) was expressed, refolded *in vitro* and purified as described.[22]

Crystallography

Crystals of SEK were grown by the sitting-drop, vapor-diffusion method in 10% (w/v) polyethylene glycol (PEG) 6000, 2 M NaCl at room temperature. A complete data set to a nominal resolution of 1.56 Å was collected at CHESS, beam line A-1 and processed using HKL2000.[31] A molecular replacement solution for SEK was found using the program PHASER with SpeI (PDB accession code 2ICI) as a search model.[32]

For SEK-hVβ5.1 co-crystallization, the two proteins were mixed in a 1:1 molar ratio at ∼10 mg/ml total protein concentration in 10 mM Tris–HCl (pH 7.5), 25 mM NaCl but, due to the relatively low affinity of the complex, no further purification of the complex was performed before crystallization. Co-crystals were grown by the hanging-drop, vapor-diffusion method in 0.1 M Mes (pH 6.0–7.0), 6–10% (w/v) PEG 20,000, at room temperature. A complete data set to a nominal resolution of 2.40 Å was collected at

NSLS, beam line X6A and processed using HKL2000.[31] A molecular replacement solution for the SEK-hVβ5.1 complex was found using the program PHASER[32] with the partially refined SEK structure and the β chain molecule of the 3A6 TCR (PDB accession code 1ZGL) as search models.

The SEK and SEK-hVβ5.1 structures were refined using REFMAC[33] and CNS,[34] respectively, interspersed with manual model building in COOT.[35] Crystallographic data collection, processing and refinement statistics are given in Table 1.

Binding analysis

Affinity measurements were made using a Biacore 3000 SPR instrument (Biacore, Piscataway, NJ). Wild-type SEK or SEK mutants were immobilized on CM5 sensor chips by standard amine coupling to an immobilization density of approximately 500 response units. TSST-1 was immobilized at an density equivalent to a negative control surface. A concentration gradient of hVβ5.1 was injected over all surfaces and the net maximal responses were recorded for steady-state analysis. Affinity values were derived by non-equilibrium regression analysis using the BiaEvaluation 4.1 software (Biacore, Piscataway, NJ).

Functional analysis

To allow for a functional readout for the SEK mutants specific for the hVβ5.1 chain used in the SEK-hVβ5.1 complex, the Jurkat T cell line JRT3-T3.5 (ATCC) was used. This cell line lacks the endogenous hVβ8.1 chain present in wild-type Jurkat T cells.[36] Recombinant hVβ5.1 was constructed essentially as described,[24] where the leader and transmembrane DNA sequences of human hVβ8.1[37] were attached to the 5′ and 3′ ends of hVβ5.1 cDNA, respectively, to allow for surface expression and pairing of hVβ5.1 with the endogenous hVα1. These modifications to the hVβ5.1 cDNA were performed by sequential megaprimer PCR reactions and the complete hVβ5.1 cDNA was cloned into the unique KpnI and BamHI sites in pBIG2i.[38] A 10 μg sample of linearized pBIG2i::hVβ5.1 was electroporated into 5×10^6 JRT3-T3.5 cells using 300 V and 950 μF, and stable transfectants were selected using increasing concentrations of hygromycin B. JRT3-T3.5 transfected with pBIG2i alone was used as a negative control. Surface expression of hVβ5.1 paired with endogenous Vα1 was confirmed using fluorescence activated cell sorting analysis with PE-conjugated anti-TCR antibody (eBioscience). Transfected JRT3-T3.5 cells (10^5) were incubated with LG-2 cells (2×10^4) to provide MHC class II, with different concentrations of the various SEK variants in a non-adherent 96-well plate for 16–18 h. Activation was monitored using ELISA for human IL-2 (BD biosciences).

For aggregation assays, LG-2 cells (1×10^5 cells/ml) were incubated with 1 μg/ml of recombinant SEK proteins in non-adherent, flat-bottomed 96-well plates and monitored for cell aggregation for 7 h. Wells were exposed to 1 μg/ml of superantigen and the percentage of cells in aggregates was assessed at 1 h intervals for 6 h. The control consisted of LG-2 cells not exposed to superantigen. The zinc-dependence of the high-affinity MHC class II binding site was tested by the addition of 1 mM (final concentration) EDTA at 2 h and subsequent addition of 2 mM (final concentration) $ZnSO_4$ at 4 h. The number of cells in aggregates was assessed as a percentage of the total number of cells in the field of view at a magnification of 100×.

Protein Data Bank accession codes

The atomic coordinates and structure factors have been deposited in the Protein Data Bank (PDB ID codes 2NTT for SEK, and 2NTS for SEK-hVβ5.1).

Acknowledgements

We thank the staffs at CHESS beam line A-1 and NSLS beam line X6A. This work was supported by a Canadian Institute of Health Research operating grant and a New Investigator award (to JKM), and by National Institutes of Health grant AI036900 (to RAM).

References

1. McCormick, J. K., Yarwood, J. M. & Schlievert, P. M. (2001). Toxic shock syndrome and bacterial superantigens: an update. *Annu. Rev. Microbiol.* **55**, 77–104.
2. Sundberg, E. J., Li, Y. & Mariuzza, R. A. (2002). So many ways of getting in the way: diversity in the molecular architecture of superantigen-dependent T-cell signaling complexes. *Curr. Opin. Immunol.* **14**, 36–44.
3. Kaul, R., McGeer, A., Norrby-Teglund, A., Kotb, M., Schwartz, B., O'Rourke, K. *et al.* (1999). Intravenous immunoglobulin therapy for streptococcal toxic shock syndrome – a comparative observational study. The Canadian Streptococcal Study Group. *Clin. Infect. Dis.* **28**, 800–807.
4. LeClaire, R. D. & Bavari, S. (2001). Human antibodies to bacterial superantigens and their ability to inhibit T-cell activation and lethality. *Antimicrob. Agents Chemother.* **45**, 460–463.
5. Li, Y., Li, H., Dimasi, N., McCormick, J. K., Martin, R., Schuck, P. *et al.* (2001). Crystal structure of a superantigen bound to the high-affinity, zinc-dependent site on MHC class II. *Immunity*, **14**, 93–104.
6. Jardetzky, T. S., Brown, J. H., Gorga, J. C., Stern, L. J., Urban, R. G., Chi, Y. I. *et al.* (1994). Three-dimensional structure of a human class II histocompatibility molecule complexed with superantigen. *Nature*, **368**, 711–718.
7. Kim, J., Urban, R. G., Strominger, J. L. & Wiley, D. C. (1994). Toxic shock syndrome toxin-1 complexed with a class II major histocompatibility molecule HLA-DR1. *Science*, **266**, 1870–1874.
8. Sundberg, E. J., Li, H., Llera, A. S., McCormick, J. K., Tormo, J., Schlievert, P. M. *et al.* (2002). Structures of two streptococcal superantigens bound to TCR beta chains reveal diversity in the architecture of T cell signaling complexes. *Structure*, **10**, 687–699.
9. Moza, B., Varma, A. K., Zhu, P., Buonpane, R. A., Herfst, C. A., Nicholson, M. J. *et al.* (2007). Structural basis of T cell receptor specificity and activation by the bacterial superantigen TSST-1. *EMBO J.* **26**, 1187–1197.
10. Li, H., Llera, A., Tsuchiya, D., Leder, L., Ysern, X., Schlievert, P. M. *et al.* (1998). Three-dimensional structure of the complex between a T cell receptor beta chain and the superantigen staphylococcal enterotoxin B. *Immunity*, **9**, 807–816.
11. Proft, T. & Fraser, J. D. (2003). Bacterial superantigens. *Clin. Expt. Immunol.* **133**, 299–306.

12. Brouillard, J.-N. P., Gunther, S., Varma, A. K., Gryski, I., Herfst, C. A., Rahman, A. K. *et al.* (2007). Crystal structure of the streptococcal superantigen SpeI and functional role of a novel loop domain in T cell activation by Group V superantigens. *J. Mol. Biol.* **367**, 925–934.
13. Wen, R., Cole, G. A., Surman, S., Blackman, M. A. & Woodland, D. L. (1996). Major histocompatibility complex class II-associated peptides control the presentation of bacterial superantigens to T cells. *J. Expt. Med.* **183**, 1083–1092.
14. Moza, B., Buonpane, R. A., Zhu, P., Herfst, C. A., Rahman, A. K., McCormick, J. K. *et al.* (2006). Long-range cooperative binding effects in a T cell receptor variable domain. *Proc. Natl Acad. Sci. USA*, **103**, 9867–9872.
15. Fields, B. A., Malchiodi, E. L., Li, H., Ysern, X., Stauffacher, C. V., Schlievert, P. M. *et al.* (1996). Crystal structure of a T-cell receptor beta-chain complexed with a superantigen. *Nature*, **384**, 188–192.
16. Abrahmsen, L., Dohlsten, M., Segren, S., Bjork, P., Jonsson, E. & Kalland, T. (1995). Characterization of two distinct MHC class II binding sites in the superantigen staphylococcal enterotoxin A. *EMBO J.* **14**, 2978–2986.
17. Hudson, K. R., Tiedemann, R. E., Urban, R. G., Lowe, S. C., Strominger, J. L. & Fraser, J. D. (1995). Staphylococcal enterotoxin A has two cooperative binding sites on major histocompatibility complex class II. *J. Expt. Med.* **182**, 711–720.
18. Petersson, K., Thunnissen, M., Forsberg, G. & Walse, B. (2002). Crystal structure of a SEA variant in complex with MHC class II reveals the ability of SEA to crosslink MHC molecules. *Structure*, **10**, 1619–1626.
19. Petersson, K., Hakansson, M., Nilsson, H., Forsberg, G., Svensson, L. A., Liljas, A. & Walse, B. (2001). Crystal structure of a superantigen bound to MHC class II displays zinc and peptide dependence. *EMBO J.* **20**, 3306–3312.
20. Li, Y., Li, H., Dimasi, N., McCormick, J. K., Martin, R., Schuck, P. *et al.* (2001). Crystal structure of a superantigen bound to the high-affinity, zinc-dependent site on MHC class II. *Immunity*, **14**, 93–104.
21. Fernandez, M. M., Guan, R., Swaminathan, C. P., Malchiodi, E. L. & Mariuzza, R. A. (2006). Crystal structure of staphylococcal enterotoxin I (SEI) in complex with a human major histocompatibility complex class II molecule. *J. Biol. Chem.* **281**, 25356–25364.
22. Li, Y., Huang, Y., Lue, J., Quandt, J. A., Martin, R. & Mariuzza, R. A. (2005). Structure of a human autoimmune TCR bound to a myelin basic protein self-peptide and a multiple sclerosis-associated MHC class II molecule. *EMBO J.* **24**, 2968–2979.
23. Buonpane, R. A., Moza, B., Sundberg, E. J. & Kranz, D. M. (2005). Characterization of T cell receptors engineered for high affinity against toxic shock syndrome toxin-1. *J. Mol. Biol.* **353**, 308–321.
24. Rahman, A. K., Herfst, C. A., Moza, B., Shames, S. R., Chau, L. A., Bueno, C. *et al.* (2006). Molecular basis of TCR selectivity, cross-reactivity, and allelic discrimination by a bacterial superantigen: integrative functional and energetic mapping of the SpeC-Vbeta2.1 molecular interface. *J. Immunol.* **177**, 8595–8603.
25. Jarraud, S., Peyrat, M. A., Lim, A., Tristan, A., Bes, M., Mougel, C. *et al.* (2001). egc, a highly prevalent operon of enterotoxin gene, forms a putative nursery of superantigens in Staphylococcus aureus. *J. Immunol.* **166**, 669–677.
26. Orwin, P. M., Leung, D. Y., Donahue, H. L., Novick, R. P. & Schlievert, P. M. (2001). Biochemical and biological properties of *staphylococcal enterotoxin K. Infect. Immun.* **69**, 360–366.
27. Prindiville, T. P., Cantrell, M. C., Matsumoto, T., Brown, W. R., Ansari, A. A., Kotzin, B. L. & Gershwin, M. E. (1996). Analysis of function, specificity and T cell receptor expression of cloned mucosal T cell lines in Crohn's disease. *J. Autoimmun.* **9**, 193–204.
28. Nakajima, T., Yamazaki, K. & Hara, K. (1996). Biased T cell receptor V gene usage in tissues with periodontal disease. *J. Periodontal Res.* **31**, 2–10.
29. McDermott, M., Kastner, D. L., Holloman, J. D., Schmidt-Wolf, G., Lundberg, A. S., Sinha, A. A. *et al.* (1995). The role of T cell receptor beta chain genes in susceptibility to rheumatoid arthritis. *Arthritis Rheum.* **38**, 91–95.
30. Bueno, C., Lemke, C. D., Criado, G., Baroja, M. L., Ferguson, S. S., Rahman, A. K. *et al.* (2006). Bacterial superantigens bypass Lck-dependent T cell receptor signaling by activating a Galpha11-dependent, PLC-beta-mediated pathway. *Immunity*, **25**, 67–78.
31. Otwinowski, Z. & Minor, W. (1997). Processing X-ray diffraction data collected in oscillation mode. *Methods Enzymol.* **276**, 307–326.
32. Storoni, L. C., McCoy, A. J. & Read, R. J. (2004). Likelihood-enhanced fast rotation functions. *Acta Crystallog. sect. D*, **60**, 432–438.
33. Murshudov, G. N., Vagin, A. A. & Dodson, E. J. (1997). Refinement of macromolecular structures by the maximum-likelihood method. *Acta Crystallog. sect. D*, **53**, 240–255.
34. Brunger, A. T., Adams, P. D., Clore, G. M., DeLano, W. L., Gros, P., Grosse-Kunstleve, R. W. *et al.* (1998). Crystallography and NMR system: a new software suite for macromolecular structure determination. *Acta Crystallog. sect. D*, **54**, 905–921.
35. Emsley, P. & Cowtan, K. (2004). Coot: model-building tools for molecular graphics. *Acta Crystallog. sect. D*, **60**, 2126–2132.
36. Weiss, A. & Stobo, J. D. (1984). Requirement for the coexpression of T3 and the T cell antigen receptor on a malignant human T cell line. *J. Expt. Med.* **160**, 1284–1299.
37. Ohashi, P., Mak, T., Elsen, P. v. d., Yanagi, Y., Yoshikai, Y., Calan, A. *et al.* (1985). Reconstitution of an active surface T3/T-cell antigen receptor by DNA transfer. *Nature*, **316**, 606–609.
38. Strathdee, C., McLeod, M. & Hall, J. (1999). Efficient control of tetracycline-responsive gene expression from an autoregulated bi-directional expression vector. *Gene*, **229**, 21–29.

Edited by I. Wilson

(Received 16 March 2007; received in revised form 10 May 2007; accepted 11 May 2007)
Available online 18 May 2007